

Sequence-specific self-assembly of positive and negative monomers with Cucurbit[8]uril linkers

Mersad Raeisi, Kondalarao Kotturi, Ian Del Valle, Jan Schulz, Paulina Dornblut, and Eric Masson

J. Am. Chem. Soc., **Just Accepted Manuscript** • DOI: 10.1021/jacs.7b13304 • Publication Date (Web): 14 Feb 2018

Downloaded from <http://pubs.acs.org> on February 14, 2018

Just Accepted

“Just Accepted” manuscripts have been peer-reviewed and accepted for publication. They are posted online prior to technical editing, formatting for publication and author proofing. The American Chemical Society provides “Just Accepted” as a service to the research community to expedite the dissemination of scientific material as soon as possible after acceptance. “Just Accepted” manuscripts appear in full in PDF format accompanied by an HTML abstract. “Just Accepted” manuscripts have been fully peer reviewed, but should not be considered the official version of record. They are citable by the Digital Object Identifier (DOI®). “Just Accepted” is an optional service offered to authors. Therefore, the “Just Accepted” Web site may not include all articles that will be published in the journal. After a manuscript is technically edited and formatted, it will be removed from the “Just Accepted” Web site and published as an ASAP article. Note that technical editing may introduce minor changes to the manuscript text and/or graphics which could affect content, and all legal disclaimers and ethical guidelines that apply to the journal pertain. ACS cannot be held responsible for errors or consequences arising from the use of information contained in these “Just Accepted” manuscripts.

Sequence-specific self-assembly of positive and negative monomers with Cucurbit[8]uril linkers

Mersad Raeisi, Kondalarao Kotturi, Ian del Valle, Jan Schulz, Paulina Dornblut and Eric Masson*

Department of Chemistry and Biochemistry, Ohio University, Athens, Ohio 45701, United States.

ABSTRACT: The self-assembly into dynamic oligomers of Cucurbit[8]uril (CB[8]), a positive ditopic Ir(III) bis-terpyridine complex, and a negative ditopic Fe(II) bis-terpyridine complex flanked by four butyrate side chains was assessed to answer a seemingly straightforward question: does CB[8] adopt a social self-sorting pattern by encapsulating both positive and negative units into a hetero-ternary complex? We showed that this is indeed the case, with CB[8] linking a positive Ir unit to a neighboring negative Fe unit whenever possible. Furthermore, the solubility of the dynamic oligomers was significantly affected by their sequence; upon addition of 0.6 – 1.2 equiv. positive Ir oligomer to its negative Fe counterpart, the predominant assembly present in solution was a mixed oligomer with a (Fe–Ir–Ir)_n sequence. Weak interactions between the negative butyrate side chains and the partially positive outer wall of CB[7] were also identified by two-dimensional nuclear magnetic resonance techniques, and resulted in a negative pK_a shift (0.10 pK_a unit) for the terminal carboxylic groups.

INTRODUCTION

The recognition properties of the cavity of Cucurbit[n]uril macrocycles (CB[n]) have been studied for more than 30 years, and the major driving forces responsible for guest encapsulation in aqueous medium, very often with extreme affinity, are now firmly established.¹⁻⁸ The ejection of water from the CB[n] cavity back to the bulk, a process that is enthalpically and entropically favorable, accounts for much of the affinity. Rigid guests, tight fits into the macrocycle cavity, and the presence of positively charged substituents that interact with the carbonyl portals of CB[n] are major affinity enhancing factors. In the latter case, binding affinities typically increase by 10³ to 10⁴-fold for each portal/positive substituent interaction.² Neutral guests,¹ including hydrocarbons, bind to CB[6],⁴ CB[7],⁹ CB[8]⁹ and to the cavity located between the inner wall of CB[8] and an auxiliary guest.¹⁰ A few years ago, we also reported that biaryl **1a** binds to CB[7] despite its net negative charge, albeit 10³ times weaker than positive analog **1b** (see Figure 1).¹¹ We are now seeking to answer the following question: how do a positive guest and a negative guest self-assemble in the presence of CB[8]? Should one expect complete social self-sorting, i.e. the exclusive formation of the hetero-ternary complex between all three units, to maximize Coulombic interactions between the positive and negative guests? Or to the contrary, are the overall charges of the guests irrelevant to the self-sorting patterns? Biaryl **1a** is one of the rare negative guests with a reported binding affinity to a member of the CB[n] family, therefore this seemingly straightforward question has never been addressed before.

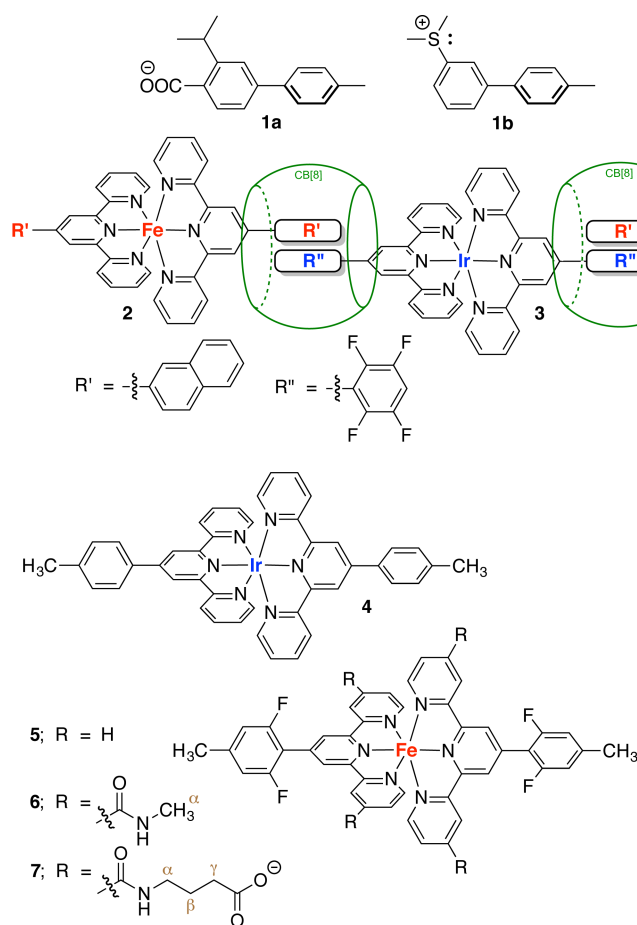


Figure 1. Biphenyl derivatives with reported binding affinities to CB[7]. CB[n]-binding metal-ligand complexes relevant to this study.

Recently, our group showed that Fe(II) and Ir(III) bis-terpyridine complexes **2** and **3**, which bear 2-naphthyl groups and

2-(2,3,5,6-tetrafluorophenyl) groups at their 4'-positions, respectively, undergo social self-sorting in the presence of CB[8], and assemble into dynamic oligomers ($2\cdot\text{CB}[8]\cdot 3\cdot\text{CB}[8]$)_n with alternating Fe and Ir metallic cores (see Figure 1).¹² The macrocycle forms hetero-ternary complexes with naphthyl units attached to the Fe(II) complex and with the tetrafluorophenyl units of the Ir(III) complex. The remarkable self-sorting pattern was attributed to favorable quadrupole-quadrupole interactions between both aromatic units inside the cavity of CB[8].¹² To answer the question asked above, we will assess the self-sorting patterns of CB[8], positive Ir(III) complex [Ir•4₂]³⁺, positive Fe(II) complexes [Fe•5₂]²⁺, [Fe•6₂]²⁺ (as controls) and doubly negative Fe(II) complex [Fe•7₂]²⁻ (see Figure 1; the preparation of all metal-ligand complexes is presented in the supporting information section). The 2,6-difluoro-4-tolyl substituent at the 4'-position of terpyridine ligands 5 – 7 was chosen to allow the monitoring of CB[n] binding by both ¹H and ¹⁹F nuclear magnetic resonance spectroscopy (NMR), the latter nucleus being particularly valuable when the terpyridine ligands are decorated with side chains resulting in more complex ¹H NMR spectra. For a clearer depiction of the intermolecular forces at play, we start by assessing the conformation of the side chains in complexes [Fe•6₂]²⁺ and [Fe•7₂]²⁻ when the difluoroaryl unit is encapsulated by CB[7]. This host is used for this portion of the study, as discrete, well-defined ternary complexes [Fe•6₂]²⁺•CB[7]₂ and [Fe•7₂]²⁻•CB[7]₂ are formed, as opposed to dynamic oligomers in the presence of CB[8].

RESULTS AND DISCUSSION

Upon addition of CB[7] to complexes Fe•L₂ (L = 5 – 7), difluoroaryl hydrogens, as well as its methyl group, underwent the expected upfield shift that characterizes encapsulation (0.95 and 0.40 ppm on average throughout the ligand 5 – 7 series; see complex [Fe•6₂]²⁺•CB[7]₂ and signals labeled 7 and 8 in Figure 2). To the contrary, hydrogens at positions 3 and 3'' of the terpyridine unit underwent a very strong downfield shift (1.13 ppm on average), an effect that we have attributed to CH...O=C hydrogen bonding with the carbonyl portal of the macrocycle.¹² ¹⁹F NMR experiments showed marked downfield shifts upon CB[7] encapsulation (2.81 ppm on average, see Figure 2). In all cases, host/guest exchanges were slow on the ¹H and ¹⁹F NMR time scales.

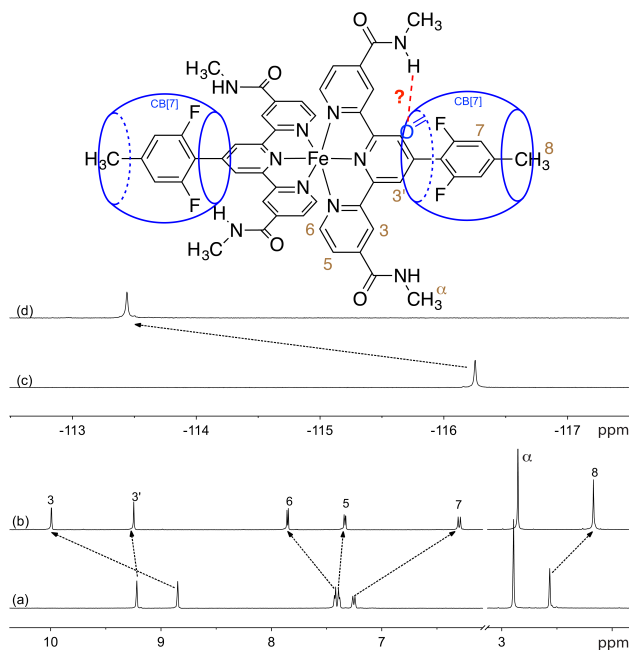


Figure 2. Complex [Fe•6₂]²⁺•CB[7]₂ highlighting the possibility for NH...O=C hydrogen bonding. ¹H NMR spectra of (a) complex [Fe•6₂]²⁺ and (b) assembly [Fe•6₂]²⁺•CB[7]₂; ¹⁹F NMR spectra of (c) complex [Fe•6₂]²⁺ and (d) assembly [Fe•6₂]²⁺•CB[7]₂.

¹H NMR spectra with water suppression were then recorded in a water/deuterium oxide mixture (9:1) to examine the possibility of hydrogen bonding between the amide side chains of complexes [Fe•6₂]²⁺ and [Fe•7₂]²⁻ and the carbonyl portal of CB[7] (see Figure 2). NH signals underwent upfield shifts (0.18 and 0.19 ppm at 25 °C in the case of complexes [Fe•6₂]²⁺ and [Fe•7₂]²⁻, respectively) upon CB[7] binding. As hydrogen bonding typically results in pronounced downfield shifts for the hydrogen nucleus of the donor,¹³⁻¹⁵ strong NH...O=C interactions are unlikely to be present in our system; we do remain cautious however, as NH...O=C hydrogen bonding resulting in upfield shifts have been observed in proteins.¹⁶ Another diagnostic test for NH...O=C hydrogen bonding that does not involve isotope labeling consists in monitoring NH chemical shifts as a function of temperature. In proteins, weak temperature gradients (−3 ± 2 ppb/K) are symptomatic of hydrogen bonding, while larger gradients (−7 ± 3 ppb/K) indicate the contrary. From a set of 793 amide protons in 14 different proteins, a 93% probability of hydrogen bonding was detected for gradients weaker than −4 ppb/K.¹⁷ NH chemical shifts were measured in complexes [Fe•6₂]²⁺, [Fe•6₂]²⁺•CB[7]₂, [Fe•7₂]²⁻ and [Fe•7₂]²⁻•CB[7]₂ at 4, 8 and 12 °C. Gradients were 4.6, 5.3, 5.3 and 3.9 ppb/K, respectively. The pair of gradients for complexes [Fe•6₂]²⁺ and [Fe•6₂]²⁺•CB[7]₂ shows unambiguously that NH...O=C hydrogen bonding is not significant, as the gradient increases in the presence of CB[7]. To the contrary, the gradient measured for assembly [Fe•7₂]²⁻•CB[7]₂ is 1.5 ppb/K weaker than its free counterpart, and falls just below the 4 ppb/K threshold. This suggests that NH...O=C hydrogen bonding between the amide side chains and the CB[7] rims, at least in some conformations of the guest, is a real possibility. We can also rule out intramolecular hydrogen bonding between the amide donors and the carboxylate acceptors of complex [Fe•7₂]²⁻, as the gradient of the latter is stronger than the one

measured for complex $[\text{Fe}\cdot\mathbf{6}_2]^{2+}$, that does not possess side chains terminated with carboxylate groups.

The plausible interaction between the CB[7] portals and the amide group of complex $[\text{Fe}\cdot\mathbf{7}_2]^{2-}$ would position the butyrate side chain in a conformation prone to interactions with the outer wall of CB[7] (see Figure 3). To test this hypothesis, we monitored the chemical shifts of the side-chain methylene groups $\alpha - \gamma$. While the signals of hydrogens at position α remain steady upon addition of CB[7] to the metal-ligand complex, hydrogens at position β and γ undergo mild upfield shifts (0.09 and 0.01 ppm, respectively, see Figure 3). While any shift should indicate proximity to the macrocycle, the former are typically upfield when hydrogens penetrate the cavity of the macrocycle, or downfield when they reside close to the carbonyl portal. Therefore in the present case, we propose that one or more guest conformations position the β -CH₂ groups, and to a lesser extent γ -CH₂ groups, near the outer methylene rim of CB[7].

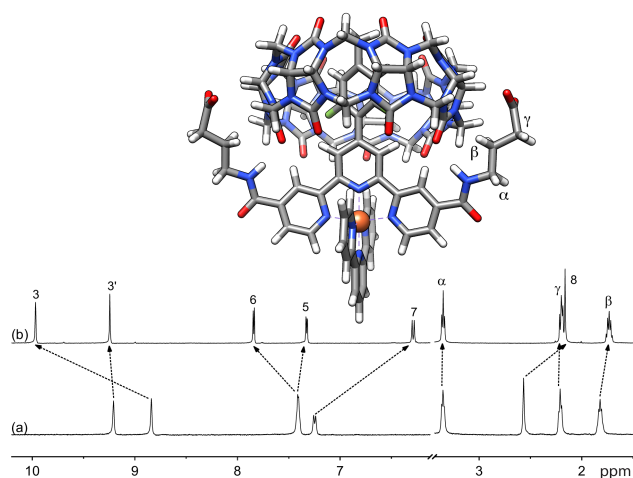


Figure 3. DFT-optimized truncated structure of a possible conformation for complex $[\text{Fe}\cdot\mathbf{7}_2]^{2-}\cdot\text{CB}[7]_2$ (TPSS-D3(BJ) functional, COSMO solvation term and def2-SVP basis sets). ¹H NMR spectra of complexes (a) $[\text{Fe}\cdot\mathbf{7}_2]^{2-}$ and (b) $[\text{Fe}\cdot\mathbf{7}_2]^{2-}\cdot\text{CB}[7]_2$.

We then carried out quantitative two-dimensional nuclear Overhauser effect spectroscopy (NOESY) experiments to determine through-space distances between the butyrate methylene groups and the closest methylene rim of CB[7]. The distances can be obtained from the growth of the cross-peaks measured upon increases in mixing times, relative to the growth of a reference cross-peak assigned to two hydrogens sitting at a known distance (see Figure 4).¹⁸⁻¹⁹ The distances between the “co-axial”²⁰ inward-pointing methylene hydrogen at the CB[7] rim closest to the α and β hydrogens of the butyrate side chain are at least 3.8 and 4.1 Å, respectively, while the distance between the “co-equatorial”²⁰ outer methylene hydrogen closest to the butyrate β -hydrogens is at least 4.3 Å. Those distances are significantly longer than those measured on a truncated DFT-optimized structure with a tight interaction between the carboxylate units and the outer wall of CB[7] (3.6, 2.3 and 2.4 Å, respectively; see Figure 3). While this structure is plausible, it is probably one of many conformations generated by the flexible butyrate side chain.

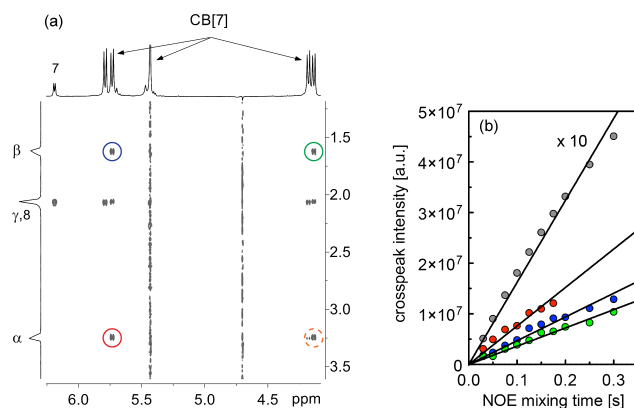


Figure 4. (a) Portion of the ¹H-¹H NOESY spectrum of complex $[\text{Fe}\cdot\mathbf{7}_2]^{2-}\cdot\text{CB}[7]_2$ with a 0.25 s mixing time. Correlations between hydrogens α and β of the butyrate side chain and the co-axial hydrogens of the CB[7] methylene rim (red and blue circles, respectively), and between hydrogens α and β and the CB[7] co-equatorial methylene hydrogens (dashed orange and green circles, respectively). (b) NOE crosspeak signal growth as a function of mixing time (same color code). Proper volume integration could not be carried out for the crosspeak highlighted with the dashed orange circle due to signal overlap. The reference NOE buildup (grey circles) corresponds to the correlation between hydrogens 3 and 3' of the terpyridine unit (see Figure 2 for numbering).

Yet, the most convincing evidence for the interaction between the outer wall of CB[7] and the terpyridine side chain of complex $[\text{Fe}\cdot\mathbf{6}_2]^{2-}$ is the impact of encapsulation on the $\text{p}K_a$ of its carboxylic groups. $\text{p}K_a$ shifts of ammonium groups interacting with, and being stabilized by the partially negative carbonyl portals of CB[7] have been thoroughly documented²¹⁻²⁹ (up to 5.2 $\text{p}K_a$ units).³⁰ If the carboxylate groups of complex $[\text{Fe}\cdot\mathbf{7}_2]^{2-}$ were to interact with and be stabilized by the partially positive outer wall of CB[7], a *negative* $\text{p}K_a$ shift for the conjugate carboxylic acid units would ensue. A positive $\text{p}K_a$ shift would be more likely if the outer wall interactions were insignificant, as the interaction between the carbonyl portals of CB[7] and the terpyridine ligands would likely stabilize and weaken the positive charge of the complex. The $\text{p}K_a$ of both free and CB[7]-bound $[\text{Fe}\cdot\mathbf{7}_2]^{2-}$ complexes were determined precisely by ¹H NMR spectroscopy from the ratios of protonated and deprotonated species in an acetic acid/sodium acetate buffer (see supporting information for details). $\text{p}K_a$'s of 4.62 (± 0.01) and 4.52 (± 0.01) were respectively obtained; the negative 0.10 (± 0.01) $\text{p}K_a$ shift thus confirms the elusive interactions between the butyrate side chains and the outer wall of CB[7]. To the best of our knowledge, this negative shift, albeit modest but clearly outside the margin of error, is unprecedented in CB[n]/guest recognition.

The impact of the metal-ligand complex total charges on CB[7] binding affinities were measured by isothermal titration calorimetry (ITC). Remarkably, they were found to be very similar (6.0 ± 0.2 , 11.1 ± 0.5 and $6.1 \pm 0.2 \times 10^6 \text{ M}^{-1}$ in the case of complexes $[\text{Fe}\cdot\mathbf{5}_2]^{2+}$, $[\text{Fe}\cdot\mathbf{6}_2]^{2+}$ and $[\text{Fe}\cdot\mathbf{7}_2]^{2+}$, respectively; see supporting information section for binding isotherms). The mere 1.9-fold preference for CB[7] binding to complex $[\text{Fe}\cdot\mathbf{6}_2]^{2+}$, which bears four amide substituents, compared to its unsubstituted analog $[\text{Fe}\cdot\mathbf{5}_2]^{2+}$ supports the lack of substantive hydrogen bonding between the CB[7] carbonylated rim and the amides of complex $[\text{Fe}\cdot\mathbf{6}_2]^{2+}$. The negligible difference in binding affinities between complex $[\text{Fe}\cdot\mathbf{7}_2]^{2-}$ and the unsubstituted analog $[\text{Fe}\cdot\mathbf{5}_2]^{2+}$ indicates

that the overall penalty for CB[7] binding to the overall negative guest $[\text{Fe}\cdot\mathbf{7}_2]^{2-}$ is counterbalanced by the stabilization of the terminal carboxylate groups by the partially positive outer methylene rim of the macrocycle. One could also argue that in aqueous medium, the major driving force for binding is the ejection of high-energy water from the cavity of CB[7], and charges at remote substituents only play a minor role, as solvation limits interactions with their partially positive surroundings. These interactions are not insignificant though, as the $\text{p}K_a$ of both free and CB[7]-bound $\text{Fe}\cdot\mathbf{7}_2$ carboxylic groups are both lower than the $\text{p}K_a$ of acetic acid (4.62 and 4.52 vs. 4.76).

While a few valuable examples of exclusion complexes have been presented in the crystalline form,³¹⁻³⁷ we showed here for the first time an interaction between a guest and the convex outer wall of CB[n] in aqueous solution. The interaction is weak though, as explained above, and should not significantly impact self-sorting patterns in the presence of CB[8].

As CB[8] encapsulates two 2,6-difluoro-4-tolyl units pertaining to two consecutive metal-ligand complexes in its cavity, consecutive additions of the macrocycle to all three metal-ligand complexes resulted in the partial formation of $[\text{Fe}\cdot\mathbf{L}_2]\cdot\text{CB}[8]\cdot[\text{Fe}\cdot\mathbf{L}_2]$ ternary complexes ($\mathbf{L} = 5 - 7$) at 0.25 equivalent CB[8], concomitantly with larger assemblies ($[\text{Fe}\cdot\mathbf{L}_2]\cdot\text{CB}[8]_{2,3}\cdot[\text{Fe}\cdot\mathbf{L}_2]$) at 0.50 - 0.75 equiv. CB[8], and finally long dynamic oligomers ($[\text{Fe}\cdot\mathbf{L}_2]\cdot\text{CB}[8]_n$) with 1.0 equivalent CB[8] (see Figure 5). We note that guest encapsulation into CB[8] dramatically increases the solubility of the host in aqueous medium. Both “ π - π stacking” interactions and CB[8] encapsulation result in large downfield shifts for fluorine nuclei (4.6 ppm), compared to experiments carried out with CB[7] (2.8 ppm on average). Signal labeled “a” and “b” at -116.11 and -116.06 ppm (see Figure 5), respectively, account for fluorine nuclei in free $[\text{Fe}\cdot\mathbf{7}_2]^{2-}$ complexes and unencapsulated atoms in complexes ($[\text{Fe}\cdot\mathbf{7}_2]\cdot\text{CB}[8]_n\cdot[\text{Fe}\cdot\mathbf{7}_2]$ ($n \geq 1$); signals “c” and “d” at -111.31 and -111.52 ppm account for encapsulated fluorine nuclei in ternary complexes $[\text{Fe}\cdot\mathbf{7}_2]\cdot\text{CB}[8]\cdot[\text{Fe}\cdot\mathbf{7}_2]$ and larger assemblies ($[\text{Fe}\cdot\mathbf{7}_2]\cdot\text{CB}[8]_{2,3}\cdot[\text{Fe}\cdot\mathbf{7}_2]$, respectively). The differentiation between both assemblies is surprising, and must indicate a significant structural change upon connection of a second CB[8] unit to ternary complex $[\text{Fe}\cdot\mathbf{7}_2]\cdot\text{CB}[8]\cdot[\text{Fe}\cdot\mathbf{7}_2]$. The formation of longer oligomer results in the broadening of the signal, with a maximum at -111.34 ppm (signal “e” in Figure 5).

Average molecular weights, and subsequently the average number of repeat metal-ligand units at a given monomer concentration (1.0 mM), were determined by diffusion-ordered NMR spectroscopy (DOSY), after calibration with all metal-ligand complexes and their CB[7]-bound assemblies prepared in this study and in earlier work¹² (see SI section for details). Molecular weights M and diffusion coefficients D are linked by the power law $D \propto M^m$. For spherical particles, the Stokes-Einstein equation affords a coefficient m equal to 1/3, as long as molecular weights are proportional to the particle volume. For non-spherical systems such as polymers, m typically ranges from 0.3 to 0.6.³⁸ Our calibration returns a coefficient m equal to 0.41 (± 0.03). Logarithms of diffusion coefficients for oligomers ($[\text{Fe}\cdot\mathbf{L}_2]\cdot\text{CB}[8]_n$ ($\mathbf{L} = 5 - 7$)) were -10.25, -10.35 and -10.30, respectively, vs. -9.48 to -9.63 as free metal-ligand complexes; this corresponds to 27, 43 and 28 repeat units at 1.0 mM monomer concentration, respectively. The longer assembly formed upon interaction of complex $[\text{Fe}\cdot\mathbf{6}_2]^{2+}$ with CB[8] compared to the other metal-ligand complexes is likely due to a higher binding affinity for the macrocycle. This trend is also observed with

CB[7], as described above. Several cases of CB[8]-assembled oligomers have been reported in the literature,³⁹⁻⁴³ a significant number of them exploiting the now iconic interaction between methylviologen and 2-naphthoxy derivatives inside CB[8].⁴⁴ However, to the best of our knowledge, $([\text{Fe}\cdot\mathbf{7}_2]^{2-}\cdot\text{CB}[8])_n$ represents the first case of an all-negative CB[8]-assembled oligomer.

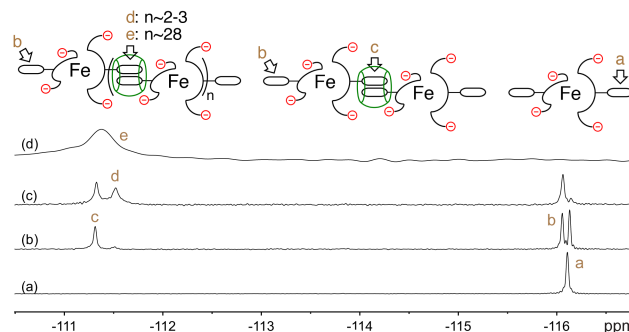


Figure 5. ^{19}F NMR spectra of complex $[\text{Fe}\cdot\mathbf{7}_2]^{2-}$ (1.0 mM) (a) in the absence of CB[8], and in the presence of (b) 0.25 equiv., (c) 0.50 equiv. and (d) 1.0 equiv. CB[8] in deuterium oxide.

The self-sorting patterns of oligomers ($[\text{Fe}\cdot\mathbf{L}_2]\cdot\text{CB}[8]_n$) once mixed with oligomer ($[\text{Ir}\cdot\mathbf{4}_2]^{3+}\cdot\text{CB}[8]_n$) could then be examined by ^1H and ^{19}F NMR spectroscopy. The latter is a particularly useful method to assess self-sorting as ^{19}F NMR signals pertaining to 2,6-difluoro-4-tolyl units in CB[8]-bound homodimers (referred to as $\mathbf{L}\cdot\mathbf{L}$; $\mathbf{L} = 5 - 7$; see Figure 6) and in CB[8]-bound heterodimers formed with the 4-tolyl substituent of ligand $\mathbf{4}$ (referred to as $\mathbf{L}\cdot\mathbf{4}$) do not overlap in most cases. $\mathbf{L}\cdot\mathbf{4}$ signals are shielded by 0.56 and 0.37 ppm compared to $\mathbf{L}\cdot\mathbf{L}$, for $\mathbf{L} = 5$ and 6, respectively; $\mathbf{7}\cdot\mathbf{4}$ and $\mathbf{7}\cdot\mathbf{4}$ signals cannot be differentiated. Fortunately, in all cases, hydrogen nuclei at positions 3 of the 2,6-difluoro-4-tolyl unit in ligands $\mathbf{5} - \mathbf{7}$, and of the 4-tolyl unit in ligand $\mathbf{4}$ resonate at different frequencies when homo- or hetero-dimers are formed inside CB[8]. They can also be used to decipher self-sorting patterns, but the complexity of ^1H NMR spectra makes the task more arduous. On average, hydrogens at position 3 of the 4-tolyl unit are deshielded by 0.26 ppm when interacting with the difluorotolyl unit in heterodimers $\mathbf{L}\cdot\mathbf{4}$ compared to homodimers $\mathbf{4}\cdot\mathbf{4}$ (see Figure 6).

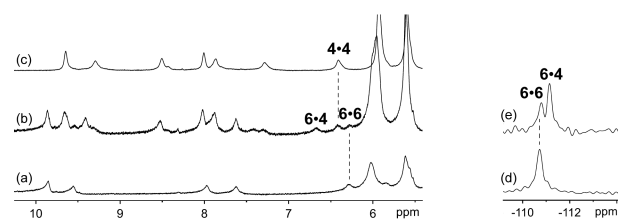
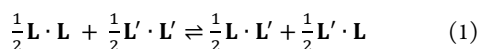


Figure 6. ^1H NMR spectra of (a) oligomer ($[\text{Fe}\cdot\mathbf{6}_2]^{2+}\cdot\text{CB}[8]_n$), (b) oligomer ($[\text{Fe}\cdot\mathbf{6}_2]^{2+}\cdot\text{CB}[8]_n$) in the presence of 1.0 equiv. oligomer ($[\text{Ir}\cdot\mathbf{4}_2]^{3+}\cdot\text{CB}[8]_n$) and (c) oligomer ($[\text{Ir}\cdot\mathbf{4}_2]^{3+}\cdot\text{CB}[8]_n$). ^{19}F NMR spectra of (d) oligomer ($[\text{Fe}\cdot\mathbf{6}_2]^{2+}\cdot\text{CB}[8]_n$) and (e) oligomer ($[\text{Fe}\cdot\mathbf{6}_2]^{2+}\cdot\text{CB}[8]_n$) in the presence of 1.0 equiv. oligomer ($[\text{Ir}\cdot\mathbf{4}_2]^{3+}\cdot\text{CB}[8]_n$). All spectra recorded in deuterium oxide; the concentration of complex $[\text{Fe}\cdot\mathbf{6}_2]^{2+}$ is 1.0 mM.

Monitoring $\mathbf{L}\cdot\mathbf{L}$ and $\mathbf{L}\cdot\mathbf{4}$ concentrations as a function of oligomer ($[\text{Ir}\cdot\mathbf{4}_2]^{3+}\cdot\text{CB}[8]_n$) concentration allows the precise quantification of the self-sorting pattern. While the terms “narcissistic” and

“social” were coined almost two decades ago⁴⁵⁻⁴⁶ to describe the exclusive formation of homo- and heterodimers, respectively, we propose here a scale that quantifies partial self-sorting patterns. We consider equilibrium (1) between a pair of homodimers ($\mathbf{L}\cdot\mathbf{L}$ and $\mathbf{L}'\cdot\mathbf{L}'$) and their corresponding heterodimers $\mathbf{L}\cdot\mathbf{L}'$ and $\mathbf{L}'\cdot\mathbf{L}$.



Its equilibrium constant K can then be readily converted into a relative free energy term ΔG (see equation 2).

$$\Delta G = -RT \ln K = -RT \ln \frac{([\mathbf{L}\cdot\mathbf{L}][\mathbf{L}'\cdot\mathbf{L}])^{1/2}}{([\mathbf{L}\cdot\mathbf{L}][\mathbf{L}'\cdot\mathbf{L}])^{1/2}} \quad (2)$$

Complexes $\mathbf{L}\cdot\mathbf{L}'$ and $\mathbf{L}'\cdot\mathbf{L}$ each account for half the total concentration of heterodimer. The free energy term can thus be readily obtained from equation 3.

$$\Delta G = -RT \ln \frac{[\mathbf{L}\cdot\mathbf{L}']^{1/2}}{([\mathbf{L}\cdot\mathbf{L}][\mathbf{L}'\cdot\mathbf{L}])^{1/2}} \quad (3)$$

We consider a self-sorting process to be fully social when $\Delta G < -2.3$ kcal/mol and fully narcissistic when $\Delta G > 2.3$ kcal/mol. Those thresholds correspond to 1:1:98 and 49:49:2 ratios of dimers $\mathbf{L}\cdot\mathbf{L}$, $\mathbf{L}'\cdot\mathbf{L}'$ and $\mathbf{L}\cdot\mathbf{L}'$, respectively, when equimolar amounts of species \mathbf{L} and \mathbf{L}' are combined with CB[8] at room temperature. A 1:1:2 ratio returns $\Delta G = 0$.

Oligomer ($[\text{Ir}\cdot\mathbf{4}_2]^{3+}\cdot\text{CB}[8]_n$) was found to undergo partially social self-sorting when allowed to scramble in the presence of oligomers ($[\text{Fe}\cdot\mathbf{5}_2]^{2+}\cdot\text{CB}[8]_n$ and $[\text{Fe}\cdot\mathbf{6}_2]^{2+}\cdot\text{CB}[8]_n$). The ratio of homo- and heterodimers could be obtained by fitting their ¹⁹F NMR signals with a sum of two Gaussian functions, and by integrating the latter (see signals **6•6** and **6•4** in Figure 6, spectra d and e). ΔG terms are -0.25 ± 0.03 and -0.29 ± 0.03 kcal/mol, respectively. The quadrupole-quadrupole interaction between 4-tolyl and 2,6-difluoro-4-tolyl units is thus preferred to the geometric mean of the tolyl/tolyl and difluorotolyl/difluorotolyl interactions. The ΔG terms also show that short amide side-chains linked to the terpyridine units do not significantly affect self-sorting patterns, at least when total charges are not affected.

To answer the question proposed in the introduction (namely, how do positive and negative building blocks self-organize in the presence of CB[8]), we added aliquots of positive oligomer ($[\text{Ir}\cdot\mathbf{4}_2]^{3+}\cdot\text{CB}[8]_n$) to negative oligomer ($[\text{Fe}\cdot\mathbf{7}_2]^{2+}\cdot\text{CB}[8]_n$), and we monitored self-sorting patterns. The concentration of oligomer ($[\text{Fe}\cdot\mathbf{7}_2]^{2+}\cdot\text{CB}[8]_n$) in solution steadily decreased after each addition, as observed by ¹H and ¹⁹F NMR spectroscopy, thereby indicating aggregation. ($[\text{Ir}\cdot\mathbf{4}_2]^{3+}\cdot\text{CB}[8]_n$) was never detected in solution, thereby confirming that the precipitate is an aggregate of scrambled oligomers containing both iron and iridium complexes. Complete precipitation of oligomer ($[\text{Fe}\cdot\mathbf{7}_2]^{2+}\cdot\text{CB}[8]_n$) was obtained in the presence of approximately 0.5 equiv. ($[\text{Ir}\cdot\mathbf{4}_2]^{3+}\cdot\text{CB}[8]_n$). A plot of the amount of ($[\text{Fe}\cdot\mathbf{7}_2]^{2+}\cdot\text{CB}[8]_n$) in solution as a function of added iridium content is linear (see Figure 7a); the slope of the linear regression (2.38 ± 0.17) represents the number of $[\text{Fe}\cdot\mathbf{7}_2]^{2+}$ units that precipitate together with each equivalent of complex $[\text{Ir}\cdot\mathbf{4}_2]^{3+}$. The composition of the precipitated oligomer is thus ($[\text{Fe}\cdot\mathbf{7}_2]^{2+}_{0.70}\cdot[\text{Ir}\cdot\mathbf{4}_2]^{3+}_{0.30}\cdot\text{CB}[8]_n$) (or a near 2:1 ratio of Fe and Ir complexes) with a net charge of -0.5 per CB[8] unit, counterbalanced by butyrate lithium counteranions. As scrambling between CB[8] and metal-terpyridine complexes is

instantaneous on the experiment time scale,¹² the precipitate is much more likely to be a social aggregate of scrambled Fe- and Ir-containing units interconnected with CB[8], than bundles of co-precipitated narcissistic ($[\text{Ir}\cdot\mathbf{4}_2]^{3+}\cdot\text{CB}[8]_n$ and $[\text{Fe}\cdot\mathbf{7}_2]^{2+}\cdot\text{CB}[8]_n$) oligomers.

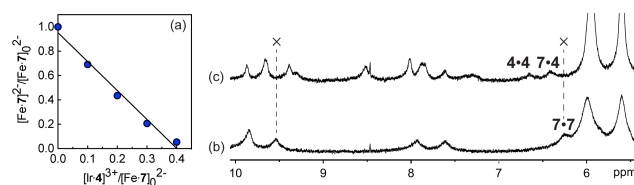


Figure 7. (a) Concentration of metal-ligand complex $[\text{Fe}\cdot\mathbf{7}_2]^{2+}$ in solution as a function of the concentration of complex $[\text{Ir}\cdot\mathbf{4}_2]^{3+}$, both relative to concentration of complex $[\text{Fe}\cdot\mathbf{7}_2]^{2+}$ in the absence of $[\text{Ir}\cdot\mathbf{4}_2]^{3+}$. ¹H NMR spectra of solutions of (b) oligomer ($[\text{Fe}\cdot\mathbf{7}_2]^{2+}\cdot\text{CB}[8]_n$), and (c) oligomer ($[\text{Fe}\cdot\mathbf{7}_2]^{2+}\cdot\text{CB}[8]_n$) in the presence of 1.0 equiv. oligomer ($[\text{Ir}\cdot\mathbf{4}_2]^{3+}\cdot\text{CB}[8]_n$).

Subsequent additions of positive oligomer ($[\text{Ir}\cdot\mathbf{7}_2]^{3+}\cdot\text{CB}[8]_n$) to the aggregate triggered the reemergence of species in solution, as showed by ¹H NMR spectroscopy (see Figure 7, spectrum c). Remarkably, the composition of the oligomer in solution remained steady up to 1.2 equiv. ($[\text{Ir}\cdot\mathbf{4}_2]^{3+}\cdot\text{CB}[8]_n$), with 31 (± 2)% of **4•4** homodimer and 69 (± 5)% of **7•4** heterodimer formation. The average composition of the oligomer is thus ($[\text{Fe}\cdot\mathbf{7}_2]^{2+}_{0.35}\cdot[\text{Ir}\cdot\mathbf{4}_2]^{3+}_{0.65}\cdot\text{CB}[8]_n$) (or a 1:2 ratio of Fe and Ir complexes this time!), with a net charge of $+1.3$ per CB[8] unit. As the concentration of oligomer ($[\text{Ir}\cdot\mathbf{7}_2]^{3+}\cdot\text{CB}[8]_n$) is further increased, more homodimer **4•4** is formed to the expense of heterodimer **7•4**. The solubility of the oligomers in water is thus minimal when their net charge per CB[8] unit is close to neutral, within the -0.5 to $+1.3$ interval. Yet the most striking feature of the self-sorting process is the absence of homodimer **7•7**, even at low concentrations of oligomer ($[\text{Ir}\cdot\mathbf{4}_2]^{3+}\cdot\text{CB}[8]_n$) (see Figure 7). Spectrum b shows the signature signal for ($[\text{Fe}\cdot\mathbf{7}_2]^{2+}\cdot\text{CB}[8]_n$) (or **7•7**) formation at 6.25 ppm, and the latter is unequivocally absent in spectrum c (see symbol “x” in Figure 7). Therefore, self-sorting is fully social. As control experiments with terpyridine ligands bearing no side-chains or neutral ones showed only partially social self-sorting with oligomer ($[\text{Ir}\cdot\mathbf{4}_2]^{3+}\cdot\text{CB}[8]_n$), one can conclude that positive metal-ligand complex $[\text{Ir}\cdot\mathbf{4}_2]^{3+}$ do exhibit a strong preference for overall negative complex $[\text{Fe}\cdot\mathbf{7}_2]^{2+}$ when undergoing CB[8] encapsulation. A 1:2 ratio of CB[8]-bound $[\text{Fe}\cdot\mathbf{7}_2]^{2+}$ and $[\text{Ir}\cdot\mathbf{4}_2]^{3+}$ units, with the Fe complex always followed by an Ir complex may either correspond to (1) a distribution of sequences $(\text{Fe}-\text{Ir})_n$, $(\text{Fe}-\text{Ir}-\text{Ir})_n$ and $(\text{Fe}-\text{Ir}-\text{Ir}-\text{Ir}-\dots)_n$, or (2) a unique $(\text{Fe}-\text{Ir}-\text{Ir})_n$ sequence. If the first scenario were to be correct, the Fe/Ir ratio in solution would steadily decrease as more oligomer ($[\text{Ir}\cdot\mathbf{4}_2]^{3+}\cdot\text{CB}[8]_n$) is added to the solution, starting at a 1:1 ratio. As discussed above, this is not the case: the Fe/Ir ratio in solution remains steady at 1:2 upon addition of 0.6 to 1.2 equiv. ($[\text{Ir}\cdot\mathbf{4}_2]^{3+}\cdot\text{CB}[8]_n$) to oligomer ($[\text{Fe}\cdot\mathbf{7}_2]^{2+}\cdot\text{CB}[8]_n$). We thus conclude that self-sorting is not only exclusively social, but it also leads to the formation of a predominant $(\text{Fe}-\text{Ir}-\text{Ir})_n$ sequence.

CONCLUSIONS

An elusive interaction between the butyrate side-chains of complex $[\text{Fe}\cdot\mathbf{7}_2]^{2+}$ and the convex outer wall of CB[7] was detected in aqueous medium. The interaction led to a subtle, yet significant,

negative pK_a shift (0.10) for the butyric acid unit when put in contact with a neighboring CB[7] host. Despite its doubly negative charge, this metal-ligand complex not only formed tight assemblies with CB[7] upon encapsulation of its 4'-substituents, but also assembled into dynamic oligomers in the presence of CB[8]. Fully social self-sorting is observed between CB[8], positive metal-ligand complex $[\text{Ir}\cdot\mathbf{4}_2]^{3+}$ and negative complex $[\text{Fe}\cdot\mathbf{7}_2]^{2-}$, which self-assemble into hetero-ternary complexes exclusively. While the addition of positive oligomer $([\text{Ir}\cdot\mathbf{4}_2]^{3+}\cdot\text{CB}[8])_n$ to negative oligomer $([\text{Fe}\cdot\mathbf{7}_2]^{2-}\cdot\text{CB}[8])_n$ triggered the precipitation of a mixed Fe/Ir aggregate in a 7:3 ratio at low Ir concentration, further enrichment in Ir oligomer content returned Fe units into solution, as part of an oligomer with a preferred $(\text{Fe}-\text{Ir}-\text{Ir})_n$ sequence.

The next step in this study consists in evaluating the impact of third party targets, such as proteins, on the self-sorting properties of these dynamic oligomers, whose sequence is expected to be altered to maximize interactions between the ligand side-chains and the target. Progress will be reported in due course.

ASSOCIATED CONTENT

Supporting Information

Preparation and characterization of metal-ligand complexes $[\text{Fe}\cdot\mathbf{L}_2]$ ($\mathbf{L} = \mathbf{5} - \mathbf{7}$), their precursors, their assemblies with CB[7] and CB[8], as well as complex $[\text{Ir}\cdot\mathbf{4}_2]^{3+}$ and oligomer $([\text{Ir}\cdot\mathbf{4}_2]^{3+}\cdot\text{CB}[8])_n$. Are also included the binding isotherms of CB[7] to complexes $[\text{Fe}\cdot\mathbf{L}_2]$, the determination of the pK_a of complexes $[\text{Fe}\cdot\mathbf{7}_2]^{2-}$ and $[\text{Fe}\cdot\mathbf{7}_2]^{2-}\cdot\text{CB}[7]_2$, and the determination of oligomer length by DOSY experiments. The Supporting Information is available free of charge on the ACS Publications website.

AUTHOR INFORMATION

Corresponding Author

* masson@ohio.edu

Notes

The authors declare no competing financial interest.

ACKNOWLEDGMENT

We are grateful to the National Science Foundation (grant CHE-1507321), the American Chemical Society Petroleum Research Fund (grant 56375-ND4) and Ohio University for their financial support. MR and KK were also supported in part by a fellowship from the Condensed Matter and Surface Science Program (CMSS) at Ohio University. We also thank Dr. Roymon Joseph for his valuable and frequent input in the course of this study, as well as Dr. Alexandar L. Hansen, from the Campus Chemical Instrument Center at The Ohio State University, for recording the DOSY and NOESY spectra discussed therein, and offering training to MR and KK.

REFERENCES

- (1) Rekharsky, M. V.; Mori, T.; Yang, C.; Ko, Y. H.; Selvapalam, N.; Kim, H.; Sobransingh, D.; Kaifer, A. E.; Liu, S.; Isaacs, L.; Chen, W.; Moghaddam, S.; Gilson, M. K.; Kim, K.; Inoue, Y. *Proc. Natl. Acad. Sci. U. S. A.* **2007**, *104*, 20737-20742.
- (2) Moghaddam, S.; Yang, C.; Rekharsky, M.; Ko, Y. H.; Kim, K.; Inoue, Y.; Gilson, M. K. *J. Am. Chem. Soc.* **2011**, *133*, 3570-3581.
- (3) Ko, Y. H.; Hwang, I.; Lee, D.-W.; Kim, K. *Isr. J. Chem.* **2011**, *51*, 506-514.

- (4) Florea, M.; Nau, W. M. *Angew. Chem., Int. Ed.* **2011**, *50*, 9338-9342.
- (5) Biedermann, F.; Uzunova, V. D.; Scherman, O. A.; Nau, W. M.; De Simone, A. *J. Am. Chem. Soc.* **2012**, *134*, 15318-15323.
- (6) Nau, W. M.; Florea, M.; Assaf, K. I. *Isr. J. Chem.* **2011**, *51*, 559-577.
- (7) Koner, A. L.; Nau, W. M. *Supramol. Chem.* **2007**, *19*, 55-66.
- (8) Ling, X.; Saretz, S.; Xiao, L.; Francescon, J.; Masson, E. *Chem. Sci.* **2016**, *7*, 3569-3573.
- (9) Lu, X.; Isaacs, L. *Angew. Chem., Int. Ed.* **2016**, *55*, 8076-8080.
- (10) Rabbani, R.; Masson, E. *Org. Lett.* **2017**, *19*, 4303-4306.
- (11) Joseph, R.; Masson, E. *Org. Biomol. Chem.* **2013**, *11*, 3116-3127.
- (12) Joseph, R.; Nkrumah, A.; Clark, R. J.; Masson, E. *J. Am. Chem. Soc.* **2014**, *136*, 6602-6607.
- (13) Berglund, B.; Vaughan, R. W. *J. Chem. Phys.* **1980**, *73*, 2037-2043.
- (14) Haushalter, K. A.; Lau, J.; Roberts, J. D. *J. Am. Chem. Soc.* **1996**, *118*, 8891-8896.
- (15) Yao, L.; Grishaev, A.; Cornilescu, G.; Bax, A. *J. Am. Chem. Soc.* **2010**, *132*, 10866-10875.
- (16) Wagner, G.; Pardi, A.; Wuethrich, K. *J. Am. Chem. Soc.* **1983**, *105*, 5948-5949.
- (17) Cierpicki, T.; Otlewski, J. *J. Biomol. NMR* **2001**, *21*, 249-261.
- (18) Baleja, J. D.; Moulton, J.; Sykes, B. D. *J. Magn. Reson.* **1990**, *87*, 375-384.
- (19) Mugridge, J. S.; Zahl, A.; van Eldik, R.; Bergman, R. G.; Raymond, K. N. *J. Am. Chem. Soc.* **2013**, *135*, 4299-4306.
- (20) Term coined by Prof. Werner Nau in private communications.
- (21) Praetorius, A.; Bailey, D. M.; Schwarzlose, T.; Nau, W. M. *Org. Lett.* **2008**, *10*, 4089-4092.
- (22) Saleh, N. i.; Koner, A. L.; Nau, W. M. *Angew. Chem., Int. Ed.* **2008**, *47*, 5398-5401.
- (23) Shaikh, M.; Dutta Choudhury, S.; Mohanty, J.; Bhasikuttan, A. C.; Nau, W. M.; Pal, H. *Chem. - Eur. J.* **2009**, *15*, 12362-12370.
- (24) Mohanty, J.; Bhasikuttan, A. C.; Nau, W. M.; Pal, H. *J. Phys. Chem. B* **2006**, *110*, 5132-5138.
- (25) Wang, R.; Macartney, D. H. *Org. Biomol. Chem.* **2008**, *6*, 1955-1960.
- (26) Wyman, I. W.; Macartney, D. H. *Org. Biomol. Chem.* **2010**, *8*, 247-252.
- (27) Saleh, N. i.; Al-Handawi, M. B.; Bufaroosha, M. S.; Assaf, K. I.; Nau, W. M. *J. Phys. Org. Chem.* **2016**, *29*, 101-106.
- (28) Gavvala, K.; Koninti, R. K.; Sengupta, A.; Hazra, P. *Phys. Chem. Chem. Phys.* **2014**, *16*, 2823-2826.
- (29) Li, S.; Yin, H.; Wyman, I. W.; Zhang, Q.; Macartney, D. H.; Wang, R. *J. Org. Chem.* **2016**, *81*, 1300-1303.
- (30) Barooah, N.; Mohanty, J.; Pal, H.; Bhasikuttan, A. C. *J. Phys. Chem. B* **2012**, *116*, 3683-3689.
- (31) Cui, X.; Zhao, W.; Chen, K.; Ni, X.-L.; Zhang, Y.-Q.; Tao, Z. *Chem. - Eur. J.* **2017**, *23*, 2759-2763.
- (32) Shen, F.-F.; Zhao, J.-L.; Chen, K.; Hua, Z.-Y.; Chen, M.-D.; Zhang, Y.-Q.; Zhu, Q.-J.; Tao, Z. *CrystEngComm* **2017**, *19*, 2464-2474.
- (33) Ni, X.-L.; Xiao, X.; Cong, H.; Zhu, Q.-J.; Xue, S.-F.; Tao, Z. *Acc. Chem. Res.* **2014**, *47*, 1386-1395.
- (34) Chen, K.; Kang, Y.-S.; Zhao, Y.; Yang, J.-M.; Lu, Y.; Sun, W.-Y. *J. Am. Chem. Soc.* **2014**, *136*, 16744-16747.
- (35) Zhang, F.; Yajima, T.; Li, Y.-Z.; Xu, G.-Z.; Chen, H.-L.; Liu, Q.-T.; Yamauchi, O. *Angew. Chem., Int. Ed.* **2005**, *44*, 3402-3407.
- (36) Gao, Z.-W.; Feng, X.; Mu, L.; Ni, X.-L.; Liang, L.-L.; Xue, S.-F.; Tao, Z.; Zeng, X.; Chapman, B. E.; Kuchel, P. W.; Lindoy, L. F.; Wei, G. *Dalton Trans.* **2013**, *42*, 2608-2615.
- (37) Chen, K.; Liang, L.-L.; Liu, H.-J.; Tao, Z.; Xue, S.-F.; Zhang, Y.-Q.; Zhu, Q.-J. *CrystEngComm* **2012**, *14*, 8049-8056.
- (38) Shimada, K.; Kato, H.; Saito, T.; Matsuyama, S.; Kinugasa, S. *J. Chem. Phys.* **2005**, *122*, 244914.
- (39) Appel, E. A.; Biedermann, F.; Rauwald, U.; Jones, S. T.; Zayed, J. M.; Scherman, O. A. *J. Am. Chem. Soc.* **2010**, *132*, 14251-14260.

1 (40) del Barrio, J.; Horton, P. N.; Lairez, D.; Lloyd, G. O.;
2 Toprakcioglu, C.; Scherman, O. A. *J. Am. Chem. Soc.* **2013**, *135*, 11760-
3 11763.

4 (41) Liu, J.; Tan, C. S. Y.; Lan, Y.; Scherman, O. A. *Macromol.*
5 *Chem. Phys.* **2016**, *217*, 319-332.

6 (42) Ma, X.; Tian, H. *Acc. Chem. Res.* **2014**, *47*, 1971-1981.

7 (43) Yin, J.-F.; Hu, Y.; Wang, D.-G.; Yang, L.; Jin, Z.; Zhang, Y.;
8 Kuang, G.-C. *ACS Macro Lett.* **2017**, *6*, 139-143.

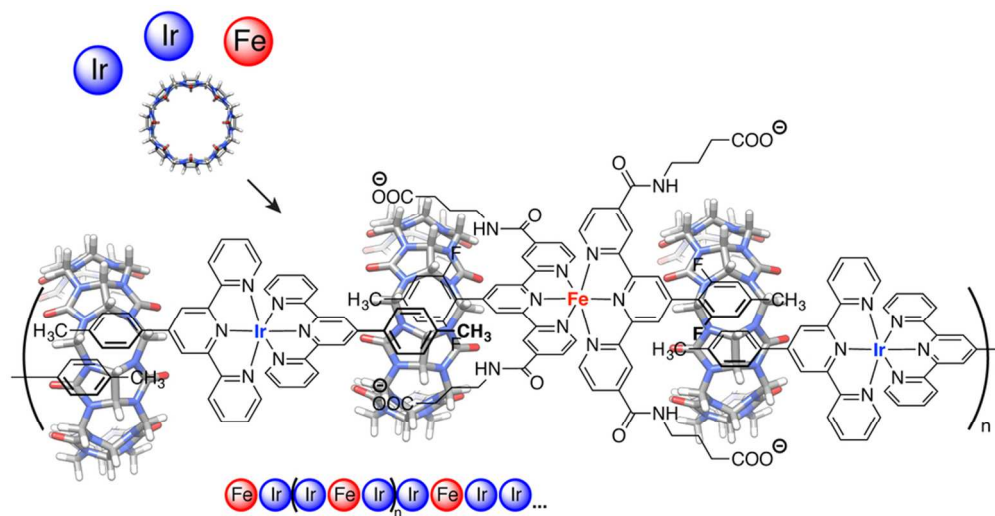
(44) Kim, H.-J.; Heo, J.; Jeon, W. S.; Lee, E.; Kim, J.; Sakamoto, S.;
Yamaguchi, K.; Kim, K. *Angew. Chem., Int. Ed.* **2001**, *40*, 1526-1529.

(45) Shivanyuk, A.; Rebek, J., Jr. *J. Am. Chem. Soc.* **2002**, *124*,
12074-12075.

(46) Taylor, P. N.; Anderson, H. L. *J. Am. Chem. Soc.* **1999**, *121*,
11538-11545.



9
10
11
12
13
14
15
16
17
18
19
20
21
22
23
24
25
26
27
28
29
30
31
32
33
34
35
36
37
38
39
40
41
42
43
44
45
46
47
48
49
50
51
52
53
54
55
56
57
58
59
60

24
25
26
27
28
29
30
31
32
33
34
35
36
37
38
39
40
41
42
43
44
45
46
47
48
49
50
51
52
53
54
55
56
57
58
59
60